Crystal Structure and Optical Characterization of Pure and Nd-Substituted Type III $KGd(PO_3)_4$

I. Parreu,[†] J. J. Carvajal,[†] X. Solans,[‡] F. Díaz,[†] and M. Aguiló*,[†]

Física i Cristal·lografia de Materials (FiCMA), Universitat Rovira i Virgili, Campus Sescelades, C/Marcel·lí i Domingo, s/n, 43007 Tarragona, Spain, and Departament de Cristal·lografia, Mineralogia i Diposits Minerals, Universitat de Barcelona, C/Martí i Franquès, s/n, 08028 Barcelona, Spain

Received September 20, 2005. Revised Manuscript Received October 28, 2005

The crystal structure of type III $KGd(PO_3)_4$ has been solved, and the related data are presented in this paper. $KGd(PO_3)_4$ (KGP) is monoclinic and has $P2_1$ as space group. Its cell parameters are $a = 7.255(4)$ Å, $b = 8.356(5)$ Å, $c = 7.934(5)$ Å, $\beta = 91.68(5)°$, and $Z = 2$. KGP is characterized by infinite polyphosphate long chains, which run along the [100] direction and are linked through gadolinium polyhedra. We determined the crystallization region of $KGd_{0.47}Nd_{0.53}(PO_3)_4$, and compared it to those of KGP and $KNd(PO_3)_4$ (KNP). The isotherms of the saturation temperature and four neighboring phases were also determined. Small Nd-substituted KGP single crystals free of macroscopic defects were successfully grown under conditions similar to those used to grow KGP and KNP crystals. Nd substitution on the structure was efficient, and its effect was analyzed. We determined the transparency windows of both KGP and KNP crystals, and evaluated the optical tensors at room temperature and 632.5 nm. Finally, we used the Kurtz method to qualitatively measure the second harmonic efficiencies of Nd-substituted KGP crystals. The values obtained for all substitutions were similar to those showed by KGP and KNP and at least to that of H_2PO_4 (KDP).

Introduction

Condensed polyphosphates of lanthanide and alkali ions with the general formula $M^{I}Ln^{III}(PO_3)_4$ crystallize into many structural types. The current nomenclature and classification of this kind of polyphosphates were first proposed by Palkina et al.[1] in 1981. The same author suggested two structural types for the polyphosphate of potassium and gadolinium: type III $KGd(PO_3)_4$ and type A $KGdP_4O_{12}$. Whereas type III was characterized by a PO_4 long-chain geometry, a PO_4 cycling geometry was typical for type A. Type III had a space group $P2_1$, $Z = 2$, $cn(M^{I}) = 8$, and $cn(Ln^{III}) = 8$, and type A had a space group $C2/c$, $Z = 4$, $cn(M^{I}) = 8$, and $cn(Ln^{III}) = 8$. The $M^{I}Ln^{III}(PO_3)_4$ structure seems to be highly dependent on the size of the alkali ion but also on that of the lanthanide when the alkali is kept fixed. From this point of view, two groups could be defined. Because gadolinium is placed in the middle of the lanthanide series, corresponding polyphosphates can crystallize into usual structural types for both the first and second groups. In fact, the type A $KGdP_4O_{12}$ structure, which is usual for the first part of the series, has been recently solved[2] by single-crystal diffraction analysis; structural type IV, which is typical for the second part of the series, has also been solved recently.[3] This structure also has a PO_4 long-chain geometry, space group $P2_1/n$, $Z = 4$, $cn(M^{I}) = 9$, and $cn(Ln^{III}) = 8$. As the type III structure has never been reported before, we solved it by single-crystal diffraction analysis.

Type III has an advantage over the other two polymorphs in that it has a noncentrosymmetrical structure, so nonlinear optical processes, such as second harmonic generation, may be allowed. Type III KGP can be easily doped with other lanthanide ions because gadolinium has a high capacity for substitution. Moreover, it expands almost isotropically with temperature, which prevents it from deforming when working above room temperature. Type III KGP is therefore regarded as a promising self-doubling host that could be used to obtain light all over the UV−vis range to low wavelengths, as the UV cutoff is about 180 nm.

In this paper, we solved for the first time the crystal structure of type III KGP and compared the crystal data with those of the isostructural KNP.[4] We also analyze the effect of substituting gadolinium with neodymium on the synthesis and on some structural and optical properties.

It has been proved that inclusion-free single crystals of both KGP[5] and KNP[6] can be successfully grown. Therefore, we determined the evolution of the crystallization region depending on the neodymium content in the KGP structure. To analyze the structural effect of Nd, we determined the evolution of the crystal cell parameters a, b, c, β, and V as a function of neodymium concentration by studying six compositions that are intermediate to the undoped composi-

* To whom correspondence should be addressed. E-mail: magdalena.aguilo@urv.net.

[†] Universitat Rovira i Virgili.

[‡] Universitat de Barcelona.

(1) Palkina, K. K.; Chudinova, N. N.; Litvin, B. N.; Vinogradova, N. V. *Izv. Akad. Nauk, Neorg. Mater.* **1981**, *17* (8), 1501.
(2) Ettis, H.; Naïli, H.; Mhiri, T. *Cryst. Growth Des.* **2003**, *3* (4), 599.
(3) Rekik, W.; Naïli, H.; Mhiri, T. *Acta Crystallogr., Sect. C* **2004**, *60*, i-50.
(4) Hong, H. Y.-P. *Mater. Res. Bull.* **1975**, *10*, 1105.
(5) Parreu, I.; Solé, R.; Gavaldà, Jna.; Massons, J.; Díaz, F.; Aguiló, M. *Chem. Mater.* **2005**, *17*, 822.
(6) Parreu, I.; Solé, R.; Gavaldà, Jna.; Massons, J.; Díaz, F.; Aguiló, M. *Chem. Mater.* **2003**, *15*, 5059.

10.1021/cm052114l CCC: $33.50
Published on Web 12/09/2005

tions. The transparency windows of KGP and KNP were measured. We also localized the principal optical directions and determined the optical tensors. We analyzed how the second harmonic generation response of powdered Nd-substituted KGP samples behaved as the neodymium concentration changed.

Experimental Section

KGP:Nd Crystal Growth. To determine the evolution of the crystallization region with the Nd^{3+} content in the KGP structure, we grew small crystals of $KGd_{1-x}Nd_x(PO_3)_4$ with solutions of 0.25, 0.50, and 0.75 neodymium at. % on a platinum disk. These crystals were grown from the corresponding self-fluxes containing the desired ratios of neodymium, gadolinium, potassium, and phosphorus oxides. About 25 solution compositions were studied in order to set the limits of the crystallization region for any material. The crystal-growth procedure was similar to that used to determine the crystallization regions of KGP and KNP (see refs 5 and 6 for further details). In this case, the axial temperature increased by about 12 K per millimeter when dipping from the surface to the crucible bottom, which was the coldest point of the volume. The cooling rate was 0.5 K/h, and the temperature dropped to about 15−20 K below the saturation temperature. The crystals grown were identified by X-ray powder diffraction analysis.

The same procedure was used to grow small crystals of KGP by varying the Nd concentration in solution from 0.02 to 75 mol %. Some of these crystals were also analyzed by X-ray powder diffraction analysis to calculate the cell parameters at different Nd atomic contents in the structure.

To obtain inclusion-free Nd-substituted KGP single crystals of suitable size for later characterizations, we used the top-seeded solution growth (TSSG)−slow cooling method. The axial gradient in the solution was 1.5 K/mm. To begin the experiments, we used the growth conditions that had been previously optimized for KGP. The solution composition was therefore Gd_2O_3:Nd_2O_3:K_2O:P_2O_5 = 6−*X*:*X*:34:60 mol %, where *X* is the Nd_2O_3 mol % in the solution; the rotation velocity was 75 rpm, the cooling rate was 0.1 K/h, and the seed orientation was *a** or *c**. A seed holder, equipped with a turbine at the bottom, was used to increase the mass transport in the solution and minimize the macroscopic defects in grown crystals. Though it was used to grow KGP:Nd, in some cases the crystals had some inclusions, especially when the neodymium content increased. To eliminate these inclusions, we discussed how the crystal growth parameters may affect the quality of the doped crystals. We previously found that the seed orientation basically affected the growth rate but not the crystal quality, so we used the same *a**- or *c**-oriented parallelepipedic seeds. The solution composition was not changed, as it has the lowest viscosity allowed in the crystallization region of KGP,[5] and was located very close to the border region. As the viscosity of the solution was similar, we also kept the rotation velocity at 75 rpm for all compositions. We therefore decided to try growing the crystals by lowering the cooling rate to 0.05 K/h. At this lower value, the crystal quality improved, and no inclusions were observed.

Neodymium Concentration Analyses. Small single crystals of Nd-substituted KGP with a Nd molar % in solution from 1 to 75 were grown using the same procedure as that in the crystallization region studies. We determined the Nd content of some of these crystals by electron probe microanalysis (EPMA) in a CAMECA SX-50 operating at a 20 kV accelerating voltage and a 100 nA electron current. We used a KGP crystal grown by us as the standard for measuring K, Gd, P, and O, and a synthetic glass (ree4) containing 4.0 mol % Nd as the standard for Nd. K and P were analyzed with PET (Pentaery thritol, 002) crystal using the line Kα. O Ka was measured with a W/Si multilayer crystal, and the Lα lines of Gd and Nd were analyzed using LIF (lithium fluoride, 200) crystal. The measurements were integrated for 10 s for all ions. The accuracy of the measurements was 1.40% for K, 1.30% for P, 1.10% for O, 1.16% for Gd, and 2.43% for Nd. For a Nd concentration below 1 mol % in solution, the measurement's accuracy decreased drastically.

X-ray Diffraction. To determine how the KGP crystallization region limits evolved with the neodymium content in the structure, we identified the Nd-substituted KGP small crystals grown by the X-ray powder diffraction technique. The patterns were recorded using Cu Kα radiation in a D5000 Siemens X-ray powder diffractometer in a $\theta-\theta$ configuration using the Bragg−Brentano geometry.

Small crystals grown from a solution composition of Gd_2O_3:Nd_2O_3:K_2O:P_2O_5 = 4−*X*:*X*:36:60 mol %, with *X* = 0.04−3, were analyzed to calculate the crystal cell parameters of the Nd-substituted KGP crystals.

The X-ray powder diffraction patterns were recorded in the 2θ range from 10 to 70° at ss = 0.03° and st = 5 s. We refined the cell parameters using the FULLPROF[7] program and the Rietveld[8] method, and the KGP structure was solved by single-crystal diffraction as the starting model.

Grown KGP and KNP crystals were analyzed by single-crystal X-ray diffraction using an Enraf−Nonius CAD-4 diffractometer; their structures were solved by the Patterson synthesis using the SHELXS97 computer program,[9] and were refined by the full-matrix least squares method using the SHELX97 program. Table 1 shows the details of the crystal data, data collection, and refinement.

Transparency Window. We measured the optical transmission of KGP and KNP in the wavelength range 0.15−10 μm. The thickness of the plate samples used was around 800 μm for both materials. The transmission in the UV−visible and NIR regions to 3.3 μm were measured using a Varian Cary 500 Scan spectrophotometer, and measurements in the IR region were made using an FTIR Midac Prospect spectrophotometer. The UV and IR cutoff values were calculated as the maximum transmission value divided by the *e* number.

Optical Tensor. Monoclinic structures show crystallographic anisotropy in all physical properties, including the optical ones. KGP and KNP are biaxial crystals whose optical properties are described by the 2-point group symmetry that arises from the $P2_1$ space group. We therefore oriented the optical frame in relation to the crystallographic one. In the monoclinic structure, one of the principal optical axes is parallel to the *b* direction, and the other two are placed in the *ac* plane. The optical ellipsoid is localized by the angle between one of the optical principal axes and one of the crystallographic axes on this plane, e.g., the *c* direction.

This angle was determined using an *ac*-oriented plate sample of KGP (1030 μm thick) and KNP (800 μm -thick), placed between two crossed glam-Taylor polarizers and illuminated under normal incidence by a He−Ne laser beam. First, we verified the crossed configuration between the polarizers when the light received by the detector was minimal. We then placed and rotated the sample

(7) Rodríguez-Carvajal, J. *Short Reference Guide for the Computer Program FULLPROF*; Laboratoire León Brillouin, CEA-CNRS: Gif sur Yvette, France, 1998.
(8) Young, R. A. *The Rietveld Method*; International Union of Crystallography Monographs on Crystallography 5; Oxford University Press: Oxford, U.K., 1995.
(9) Sheldrick, G. M. *SHELXS97 and SHELX97*; University of Göttingen: Göttingen, Germany, 1997.

Table 1. Crystal Data, Data Collection, and Refinement of $KGd(PO_3)_4$ and $KNd(PO_3)_4$

	$KGd(PO_3)_4$	$KNd(PO_3)_4$
	Crystal Data	
fw	512.23	499.22
Mo Kα radiation (λ, Å)	0.71069	0.71069
space group	monoclinic, $P2_1$	monoclinic, $P2_1$
no. of reflns	25	25
θ range (deg)	12−21	12−21
a (Å)	7.255(4)	7.2860(10)
b (Å)	8.356(5)	8.4420(10)
c (Å)	7.934(5)	8.0340(10)
μ (mm^{-1})	8.062	6.391
β (deg)	91.68(5)	92.170(10)
V ($Å^3$)	480.80(5)	493.80(11)
Z	2	2
color	colorless	purple
dimension	equidimensional	equidimensional
T (K)	293(2)	293(2)
diameter (mm)	0.2	0.2
D_x (Mg m^{-3})	3.538	3.358
D_m	not measured	not measured
	Data Collection	
R_{int}	0.0350	0.0386
ω−2θ scan, θ_{max} (deg)	29.92	29.95
Abs corr: spherical	$h = -10 \rightarrow 10$, $k = 0 \rightarrow 11$, $l = 0 \rightarrow 10$	$h = -10 \rightarrow 10$, $k = 0 \rightarrow 11$, $l = 0 \rightarrow 11$
no. of measured reflns	1834	1617
no. of independent reflns	1474	1525
no. of reflections with $I > 2\sigma(I)$	1437	1520
	Refinement	
refinement on F^2R [$F^2 > 2\sigma(F^2)$]	0.0675	0.0386
$wR(F^2)$[a]	0.1560	0.1002
$\Delta\rho_{max}/\Delta\rho_{min}$ (e $Å^{-3}$)	0.334/−0.480	0.583/−0.241
extinction correction method	none	none
S	1.168	1.089
no. of reflns	1474	1525
162 no. of params	162	162
Flack absolute struct param	−0.01(3)	0.00(2)
$(\Delta/\sigma)_{max}$	0.008	0.000

[a] From *International Tables for Crystallography, Vol. C.*: $w = 1/[\sigma^2(F_o^2) + (0.1295P)^2 + 1.1201P]$, with $P = (F_o^2 + 2F_c^2)/3$ for $KGd(PO_3)_4$, and $w = 1/[\sigma^2(F_o^2) + (0.0917P)^2 + 0.0000P]$, with $P = (F_o^2 + 2F_c^2)/3$ for $KNd(PO_3)_4$.

until the measured transmitted beam again reached a minimum, which requires the principal optical direction and the direction of the laser beam polarization to coincide.

We measured the refractive indices corresponding to the principal optical axes at 632.8 nm and room temperature for both KGP and KNP in order to determine the optical tensor under these conditions. The minimum-deviation method with a slight modification was used for this.[10] Two semiprisms were cut and polished with an angle of about 22.5° between faces, one of which was a principal plane (Np−Ng and Np−Nm). The first face was illuminated by an unpolarized laser beam under normal incidence. The prism was then rotated until a normal incidence on the second face (the principal plane) was reached. In this configuration, the beam partially reflects and returns along the same path as the incident beam. So, the path of the laser beam has a symmetrical configuration and deviates minimally throughout the prism. The anisotropic behavior of the crystals allows two beams with orthogonal polarizations to propagate in the crystal, and allows the refractive indices in these directions to be measured. Because the second face was a principal plane, we measured the refractive indices corresponding to principal axes. Thus, we measured n_p and n_g with one prism and n_p and n_m with the other. Note that as n_p was measured twice, it provides an estimate of the error in the measurements. This error is limited by the encoder accuracy, which is 10^{-3}.

Second Harmonic Generation (SHG) Measurements. We evaluated the second harmonic generation response of the Nd-substituted KGP crystals using the Kurtz method.[11] The powdered samples with a uniform particle size between 5 and 20 μm were uniformly packed, and were placed in a 2 mm thick quartz cell. Samples were irradiated using a laser beam of 1064 nm generated by a pulsed Nd:YAG solid-state laser.

We measured the energy reflected by the sample to estimate the incident power. Using a silicon PIN, we also measured the energy of the radiation it emitted. The frequency of this radiation was twice that of the incident one. We estimated the second harmonic efficiency of the sample from the ratio between these signals, which was calculated from an average of more than 100 laser shots. We compared this efficiency with that of KDP,[12] which is a well-known nonlinear optical material.

Results and Discussion

Crystallization Region of $KGd(PO_3)_4$ and $KNd(PO_3)_4$. We determined the evolution of the crystallization region limits of the type III phase from KGP to KNP in the ternary system of their corresponding oxide, Ln_2O_3, with Ln = Gd, Nd, K_2O, and P_2O_5. Figure 1 shows the crystallization region of the intermediate $KGd_{0.47}Nd_{0.53}(PO_3)_4$ in relation to those of $KGd(PO_3)_4$[5] and $KNd(PO_3)_4$.[6] The saturation temperature isotherms and SEM images of the neighboring phases

(10) Solé, R.; Nikolov, V.; Vilalta, A.; Carvajal, J. J.; Massons, J.; Gavaldà, Jna.; Aguiló, M.; Díaz, F. *J. Mater. Res.* **2002**, *17* (3), 563.
(11) Kurtz, S. K.; Perry, T. T. *J. Appl. Phys.* **1968**, *39*, 3798.
(12) Dmitriev, V. G.; Gurzadyan, G. G.; Nikogosyan, D. N. *Handbook of Nonlinear Optical Materials*; Springer-Verlag: Dusseldorf, Germany, 1991.

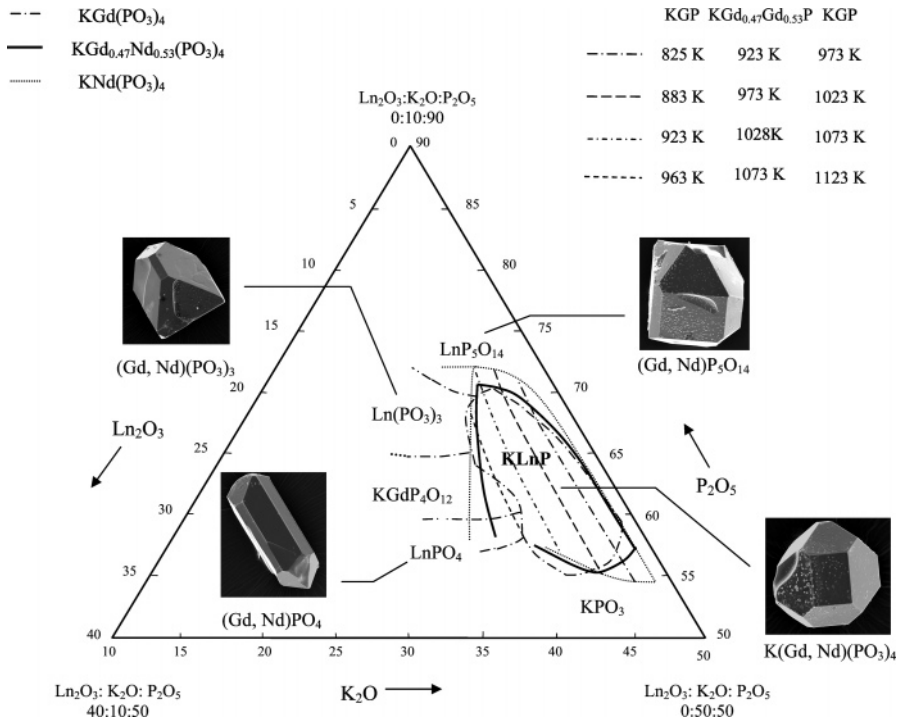

Figure 1. Crystallization region of $KGd_{0.47}Nd_{0.53}(PO_3)_4$ and those corresponding to $KGd(PO_3)_4$ and $KNd(PO_3)_4$ with saturation temperature isotherms in the $Ln_2O_3-K_2O-P_2O_5$ system, Ln = Gd, $Gd_{0.47}Nd_{0.53}$, and Nd. SEM images of $KGd_{0.5}Nd_{0.5}(PO_3)_4$ and neighboring phases.

identified were added. We knew from a previous paper[5] that the gadolinium ion had a high capacity for substitution by any other lanthanide ion because of its position in the lanthanide series, which led to a more irregular crystallization region in comparison with that of KNP. However, the crystallization region of the intermediate $KGd_{0.5}Nd_{0.5}(PO_3)_4$ is more similar to that of KNP than to that of KGP. The region has nearly the same shape, and neither the polymorph phase in the cycling geometry KLn_4O_{12} nor the mixture of orthorhombic/monoclinic $Ln(PO_3)_3$ was found.

When we compared the three crystallization regions, we found that the $P2_1$ phase crystallized in a longer extension when the neodymium concentration in the structure increased. The crystallization region limits of $KGd_{0.47}Nd_{0.53}(PO_3)_4$ were therefore placed between those of KGP and KNP. However, in the K_2O-richer zone of the phase diagram, the $[Gd_{0.47}Nd_{0.53}]O_3/K_2O$ limit coincided for all of them. Above this limit, which has a molar ratio of 3/97, the solution is so viscous that no crystal can grow. Below this limit, and up to a molar ratio of 22/78, the crystallization region is extended. Throughout these limits, $KGd_{0.47}Nd_{0.53}(PO_3)_4$ crystallizes between a P_2O_5 concentration of approximately 55 and 70 mol %. The isoconcentrational lines of $[Gd_{0.47}Nd_{0.53}]_2O_3/K_2O$ are roughly parallel to the saturation temperature isotherms, which increase from 923 to 1073 K. These temperatures are placed between those of KGP and KNP.

The four neighboring phases identified are KPO_3, $LnPO_4$,[13,14] $Ln(PO_3)_3$-orthorombic,[15,16] and $LnPO_5O_{14}$,[16,17] with Ln = Gd, (Gd,Nd), and Nd. KPO_3 crystallizes above the crystallization region and $LnPO_5O_{14}$ further above it. In the Ln_2O_3-richest zone, the other two phases are identified as $LnPO_4$ for low P_2O_5 concentrations and $Ln(PO_3)_3$ for high ones.

Crystal Structure of $KGd(PO_3)_4$ and $KNd(PO_3)_4$. The structure of KGP was solved for the first time in the present paper, and it was compared to that of the isostructural KNP, whose structure we have previously solved and which is in good agreement with that solved by Hong in 1975.[4] Both structures are monoclinic, and have $P2_1$ as its space group. The cell parameters for KGP are $a = 7.255(4)$ Å, $b = 8.356(5)$ Å, $c = 7.934(5)$ Å, $\beta = 91.68(5)°$, and $Z = 2$; those for KNP are $a = 7.2860(10)$ Å, $b = 8.4420(10)$ Å, $c = 8.0340(10)$ Å, $\beta = 92.170(10)°$, and $Z = 2$. All the KNP cell parameters are larger than the KGP ones, as expected, because the ionic radius of Nd^{3+} is slightly larger than the corresponding radius of Gd^{3+} (0.995 and 0.938 Å, respectively). The atomic coordinates, mean atomic lengths, and anisotropic thermal displacement parameters are shown in Tables 2−4.

The crystal cell of KGP and that of the isostructural KNP contain one structural position for gadolinium and potassium, four positions for phosphorus, and twelve inequivalent positions for oxygen. All atomic positions are doubled by the 2-fold screw axis parallel to [010]. The phosphate atoms are four-coordinated with the nearest oxygen atoms to form PO_4 tetrahedra. These tetrahedra are self-linked by sharing two of their vertexes to form chains, which define the type III structure. The basic unit of these chains is made of four PO_4 tetrahedra, and repeats by periodicity to generate the

(13) Mullica, D. F.; Grossie, D. A., Boatner, L. A. *Inorg. Chim. Acta* **1985**, *109*, 105.
(14) Ni, X.-Y.; Hughes, J. M.; Mariano, A. N. *Am. Mineral.* **1995**, *80*, 21.
(15) Melnikov, P. P.; Komissarova, L. N.; Butuzova, T. A. *Izv. Akad. Nauk, Neorg. Mater.* **1981**, *17* (11), 2110.
(16) Hong, H. Y.-P. *Acta Crystallogr., Sect. B* **1974**, *30*, 468.
(17) Bagieu-Beucher, M.; Doc, T. Q. *Bull. Soc. Fr. Mineral. Crystallogr.* **1970**, *93*, 505.

Table 2. Atomic Coordinates and Equivalent Isotropic Displacement Parameters of $KGd(PO_3)_4$ and $KNd(PO_3)_4$

atom	*x*	*y*	*z*	*U*(eq)	atom	*x*	*y*	*z*	*U*(eq)
Gd	0.2376(1)	0.2500(2)	0.2426(1)	0.016(1)	Nd	0.2349(1)	0.2500(1)	0.2422(1)	0.017(1)
K	0.7360(5)	0.0531(6)	0.2724(4)	0.031(1)	K	0.7268(3)	0.0543(3)	0.2808(2)	0.038(1)
P1	0.1010((5)	0.8295(6)	0.1005(4)	0.027(1)	P1	0.1031(2)	0.8304(3)	0.1037(2)	0.018(1)
P2	0.4396(6)	0.6181(6)	0.0976(5)	0.025(1)	P2	0.4342(3)	0.6280(2)	0.0979(2)	0.018(1)
P3	0.6179(5)	0.4973(6)	0.3980(4)	0.027(1)	P3	0.6220(2)	0.4965(2)	0.3959(2)	0.017(1)
P4	−0.0053(5)	0.1062(5)	0.6177(5)	0.022(1)	P4	0.0006(3)	0.1013(3)	0.6196(2)	0.018(1)
O1	0.0949(16)	0.9888(16)	0.1698(14)	0.038(2)	O1	0.0847(8)	0.9901(7)	0.1734(7)	0.024(1)
O2	0.6923(16)	0.2811(16)	0.8881(13)	0.040(3)	O2	0.6881(8)	0.2808(6)	0.8761(7)	0.025(1)
O3	0.0078(16)	0.2033(13)	0.7842(12)	0.028(2)	O3	0.0105(9)	0.2072(8)	0.7845(8)	0.030(1)
O4	0.8300(20)	−0.0100(20)	0.6154(17)	0.036(3)	O4	0.8294(7)	0.0028(8)	0.6153(7)	0.023(1)
O5	0.6810(20)	0.9870(20)	0.9231(17)	0.034(3)	O5	0.6830(9)	0.9837(8)	0.9297(7)	0.024(1)
O6	0.4320(20)	0.1770(2)	0.0337(18)	0.040(3)	O6	0.4313(9)	0.1527(9)	0.0334(8)	0.032(1)
O7	0.0357(18)	0.1895(18)	0.4675(16)	0.026(2)	O7	0.0266(9)	0.2072(7)	0.4714(8)	0.026(1)
O8	0.1779(16)	−0.0139(15)	0.6581(14)	0.036(2)	O8	0.1687(7)	−0.0119(6)	0.6552(6)	0.020(1)
O9	0.4476(19)	0.1250(19)	0.7221(15)	0.042(3)	O9	0.4608(9)	0.1344(7)	0.7263(7)	0.024(1)
O10	0.5344(15)	0.3315(14)	0.3539(13)	0.029(2)	O10	0.5377(8)	0.3441(7)	0.3448(7)	0.025(1)
O11	0.9620(15)	0.3054(15)	0.0769(13)	0.031(2)	O11	0.9635(7)	0.2975(7)	0.0680(6)	0.023(1)
O12	0.3935(16)	0.0495(15)	0.4235(14)	0.036(2)	O12	0.3858(8)	0.0558(7)	0.4277(6)	0.023(1)

Table 3. Selected Interatomic Distances (Å) in $KGd(PO_3)_4$ and $KNd(PO_3)_4$

			$KGd(PO_3)_4$				
P1−O1	1.441(12)	P3−O12	1.486(11)	Gd−O6	2.292(15)	K−O12	2.790(12)
P1−O11	1.480(11)	P3−O10	1.498(14)	Gd−O4	2.361(16)	K−O1	2.803(12)
P1−O2	1.553(12)	P3−O9	1.548(12)	Gd−O7	2.396(13)	K−O10	2.833(12)
P1−O3	1.617(11)	P3−O8	1.562(11)	Gd−O10	2.402(12)	K−O4	2.834(14)
P2−O5	1.408(16)	P4−O7	1.419(13)	Gd−O11	2.405(11)	K−O5	2.844(13)
P2−O6	1.499(15)	P4−O4	1.538(16)	Gd−O12	2.458(12)	K−O7	2.868(15)
P2−O9	1.628(13)	P4−O3	1.551(10)	Gd−O5	2.461(15)	K−O6	3.044(17)
P2−O2	1.671(13)	P4−O8	1.688(13)	Gd−O1	2.477(13)	K−O11	3.113(11)
			$KNd(PO_3)_4$				
P1−O1	1.486(6)	P3−O10	1.477(6)	Nd−O6	2.391(6)	K−O12	2.791(5)
P1−O11	1.471(5)	P3−O12	1.506(5)	Nd−O11	2.413(5)	K−O4	2.796(6)
P1−O2	1.580(6)	P3−O8	1.596(5)	Nd−O12	2.448(6)	K−O1	2.829(6)
P1−O3	1.622(6)	P3−O9	1.624(6)	Nd−O7	2.457 (5)	K−O10	2.864 6)
P2−O6	1.482 6)	P4−O4	1.498 6)	Nd−O10	2.457(6)	K−O5	2.889 6)
P2−O5	1.499 7)	P4−O7	1.506(6)	Nd−O4	2.475(7)	K−O7	2.921(8)
P2−O9	1.581(6)	P4−O8	1.571(5)	Nd−O5	2.494(6)	K−O6	2.992(8)
P2−O2	1.586(5)	P4−O3	1.597(6)	Nd−O1	2.505(6)	K−O11	3.214(6)

zigzag long chains along the *a*-crystallographic direction (Figure 2). The chains are joined by sharing the other two vertexes with the Gd^{3+} and K^+ atoms. The intrachain P−O bond distances are larger than the interchain ones, so the PO_4 tetrahedra are slightly distorted. The distortion parameter, defined as $\Delta d = {}^1/_4\Sigma_{n=1,4}[(d_n - \langle d\rangle)/\langle d\rangle]^2$, where the d_n values are the different P−O distances in the tetrahedra and $\langle d\rangle$ is the mean P−O distance, is relatively high. The values for P_1, P_2, P_3, and P_4 phosphorus tetrahedra (Figure 3), are 1.79×10^{-3}, 4.58×10^{-3}, 4.48×10^{-4}, and 3.71×10^{-3}.

The gadolinium atom is eight-coordinated with oxygen atoms to form a distorted dodecahedra. These GdO_8 polyhedra are isolated from each other because they share O atoms only with the PO_4 tetrahedra to join the chains. They are surrounded by four other GdO_8 polyhedra with large distances of about 7 Å (Figure 3). The potassium ion is also eight-coordinated with the largest distances in the structure, so it is weakly linked to the crystal lattice. It is placed close to the canals defined along the [010] direction in the $[Gd(PO_3)_4]^-$ structure (Figure 3). The Gd^{3+} and K^+ atoms alternate with a zigzag arrangement parallel to the phosphate chains.

Nd^{3+} Substitution in $KGd(PO_3)_4$. The chemical compositions of the crystals obtained from solutions of 1, 5, 10, 25, 50, and 75 mol % Nd_2O_3 were analyzed by EPMA. Table 5 shows the neodymium distribution coefficients in the structure, defined as $K_{Nd} = ([Nd]/[Nd]+[Gd])_{crystal}/([Nd]/[Nd]+[Gd])_{solution}$. They are in all cases close to 1, because the ionic radius of Nd^{3+} is only around 6% smaller than that of Gd^{3+}. Figure 4 shows the linear relationship between the average change in each cell parameter ($\Delta Y/Y$) and the neodymium concentration in crystal. Whereas the *a*, *b*, *c*, and *V* parameters increase as the Nd concentration increases, the β angle decreases slightly. The values corresponding to each composition are listed in Table 5.

Transparency Window. Figure 5 shows the transparency windows of KGP (panel a) and KNP (panel b). The IR cutoff wavelength is around 4 μm for both materials because of

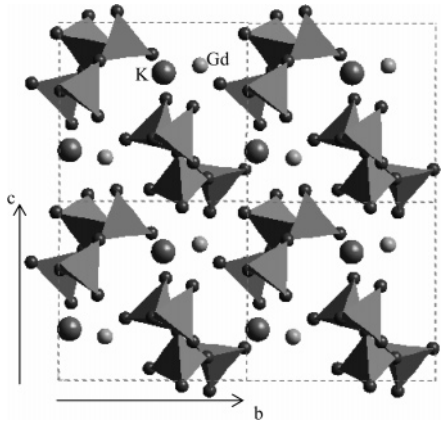

Figure 2. Zigzag arrangement of the PO_4 long chains along [100] in a projection parallel to this direction.

Table 4. Anisotropic Displacement Parameters (Å²) of $KGd(PO_3)_4$ and $KNd(PO_3)_4$

atom	U_{11}	U_{22}	U_{33}	U_{23}	U_{13}	U_{12}
			$KGd(PO_3)_4$			
Gd	0.014(1)	0.021(1)	0.014(1)	0.001(1)	−0.001(1)	−0.001(1)
K	0.028(2)	0.037(2)	0.029(1)	−0.002(2)	−0.004(1)	−0.001(1)
P1	0.023(2)	0.035(2)	0.024(2)	0(1)	−0.003(1)	−0.002(1)
P2	0.0241(2)	0.032(2)	0.017(2)	0.001(1)	0(1)	−0.002(2)
P3	0.023(2)	0.036(1)	0.022(1)	0(1)	−0.002(1)	0.002(1)
P4	0.020(2)	0.030(2)	0.017(1)	0.001(1)	−0.001(1)	−0.002(1)
O1	0.038(6)	0.038(5)	0.036(5)	−0.006(5)	−0.010(5)	0.003(5)
O2	0.030(5)	0.059(7)	0.030(4)	0.002(5)	0(4)	0(6)
O3	0.030(5)	0.033(4)	0.022(4)	−0.003(4)	0.001(4)	0.003(4)
O4	0.032(6)	0.042(6)	0.035(6)	0.002(6)	0(5)	−0.004(6)
O5	0.036(6)	0.038(6)	0.029(6)	−0.006(5)	0(5)	0.006(5)
O6	0.044(8)	0.051(8)	0.025(6)	−0.007(6)	0.006(5)	−0.002(7)
O7	0.028(6)	0.031(5)	0.019(5)	0.003(4)	0(4)	−0.005(5)
O8	0.027(5)	0.041(5)	0.041(6)	0(5)	−0.002(4)	−0.007(5)
O9	0.038(7)	0.057(7)	0.032(5)	−0.005(6)	−0.006(5)	0.010(6)
O10	0.025(5)	0.035(5)	0.026(5)	0(4)	−0.004(4)	0.007(4)
O11	0.026(5)	0.041(5)	0.026(5)	0.0011(4)	0(4)	0.001(4)
O12	0.028(5)	0.044(5)	0.036(6)	0.0015(5)	−0.003(4)	0.001(5)
			$KNd(PO_3)_4$			
Nd	0.017(3)	0.017(1)	0.018(1)	0(1)	0.003(1)	0(1)
K	0.028(1)	0.060(1)	0.027(1)	0.001(1)	0.007(1)	0.008(1)
P1	0.018(1)	0.014(1)	0.020(1)	0.001(1)	0.002(1)	0(1)
P2	0.018(1)	0.015(1)	0.022(1)	−0.001(1)	0.005(1)	0.001(1)
P3	0.015(1)	0.016(1)	0.020(1)	0(1)	0.004(1)	−0.001(1)
P4	0.019(1)	0.016(1)	0.021(1)	−0.001(1)	0.006(1)	0(1)
O1	0.023(3)	0.021(2)	0.030(2)	−0.005(2)	0.011(2)	−0.001(2)
O2	0.020(2)	0.018(2)	0.036(2)	0.002(1)	0(2)	−0.003(2)
O3	0.028(3)	0.031 (3)	0.032(3)	−0.010(2)	0.007(2)	0.003(2)
O4	0.013(2)	0.024 (3)	0.032(3)	−0.007(2)	0.006(2)	−0.003(2)
O5	0.026(3)	0.019 (3)	0.027(3)	−0.003(2)	−0.001(2)	0.001(2)
O6	0.023(3)	0.033 (3)	0.040(3)	0(3)	0.023(2)	−0.004(3)
O7	0.024(3)	0.015 (2)	0.039(3)	0.004(2)	0.020(2)	0.004(2)
O8	0.016(2)	0.016(2)	0.028(2)	0.005(2)	0.002(2)	0.007(2)
O9	0.032(3)	0.012(2)	0.026(2)	−0.002(2)	−0.008(2)	0.004(2)
O10	0.024(2)	0.021(2)	0.030(3)	0.001(2)	0.004(2)	−0.006(2)
O11	0.015(2)	0.033(3)	0.020(2)	−0.005(2)	−0.001(2)	0.007(2)
O12	0.027(3)	0.026(2)	0.016(2)	−0.005(2)	0.005(2)	0.004(2)

the absorption resonance of the P−O linkage. These crystals have a large transparency window that extends from approximately 180 nm to this wavelength. This low UV cutoff wavelength constitutes another important feature of these crystalline materials, especially when combined with their noncentrosymmetrical structures to allow the second and third harmonics of very near-IR beams. The strong absorptive bands in the KNP transmission spectrum are due to the resonance transmissions between manifolds of Nd^{3+}, which has a high concentration in this structure.

Optical Tensor. The optical frames of KGP and KNP crystals were oriented. We found a minimum transmission when the plate sample, with *b* positive toward us, was rotated clockwise 37.3 and 35.4° from the *c* direction for KGP and KNP, respectively. The second principal optical direction in the *ac* plane was therefore placed at 39.1 and 37.6° from the *a* direction for KGP and KNP, respectively.

We measured the refraction indices along the optical principal directions previously determined at 632.5 nm. In this way we were able to identify these directions as N_p, N_m, and N_g and draw the optical ellipsoid, which is shown in Figure 6 for KGP (panel a) and KNP (panel b). We found that the principal optical direction with the highest value of refraction index, N_g, was at 37.3° clockwise from the *c* direction, and the *b* direction corresponded to N_p. We can use these measurements to write the optical tensor at this

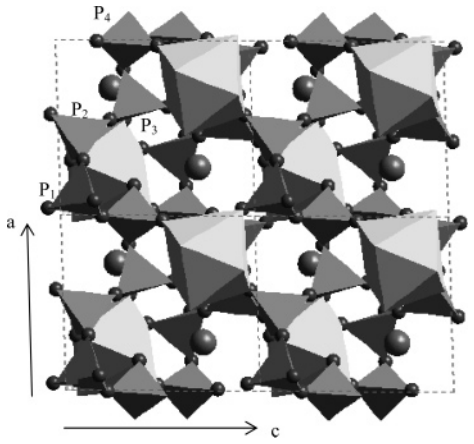

Figure 3. View of the GdO_8 dodecahedra linking the phosphate chains and the potassium atoms near the canals in the $[Gd(PO_3)_4]^-$ frame. Projection parallel to [010].

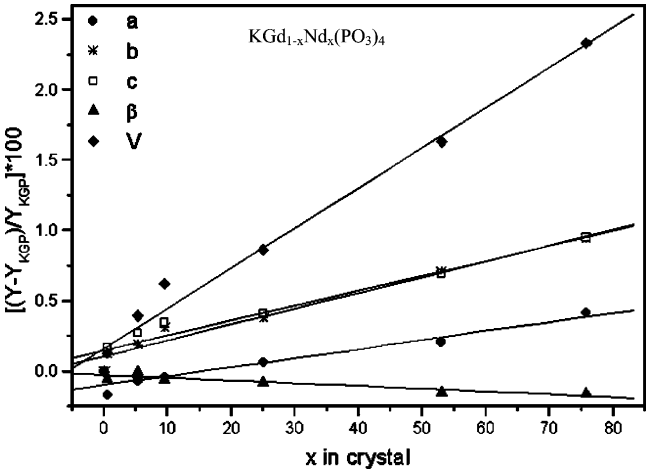

Figure 4. Relative evolution of the cell parameters and unit cell volume of $KGd_{1-x}Nd_x(PO_3)_4$ vs neodymium concentration.

Table 5. Neodymium Distribution Coefficients and Cell Parameter Values for Each Nd Concentration (in atomic %)

at. % Nd in solution	at. % Nd in crystal	K_{Nd}	*a* (Å)	*b* (Å)	*c* (Å)	*β* (deg)	*V* (Å³)
0.5	0.66	1.33	7.270(1)	8.390(1)	7.968(1)	91.67(1)	485.80
1	1.09	1.09	7.270(1)	8.391(1)	7.969(1)	91.66(1)	485.93
5	5.32	1.06	7.269(1)	8.396(1)	7.977(1)	91.72(1)	486.62
10	9.47	0.95	7.273(1)	8.406(1)	7.982(1)	91.77(1)	487.76
25	24.92	0.99	7.277(1)	8.412(1)	7.988(1)	91.85(1)	488.72
50	52.98	1.06	7.283(1)	8.440(1)	8.010(1)	91.98(1)	492.06
75	75.75	1.01	7.285(1)	8.439(1)	8.030(1)	92.02(1)	493.75

wavelength and at room temperature

$$n_{ij\ (KGP)} = \begin{pmatrix} 1.592 & 0 & 0 \\ 0 & 1.604 & 0 \\ 0 & 0 & 1.609 \end{pmatrix}$$

$$n_{ij\ (KNP)} = \begin{pmatrix} 1.596 & 0 & 0 \\ 0 & 1.586 & 0 \\ 0 & 0 & 1.602 \end{pmatrix}$$

Second Harmonic Generation Efficiency. We measured, as previously described, the SHG efficiency (η) of $KGd(PO_3)_4$, $KGd_{0.75}Nd_{0.25}(PO_3)_4$, $KGd_{0.47}Nd_{0.53}(PO_3)_4$, $KGd_{0.24}Nd_{0.76}(PO_3)_4$, and $KNd(PO_3)_4$, and compared them with that of KDP. For all compositions, the value of η/η_{KDP} was

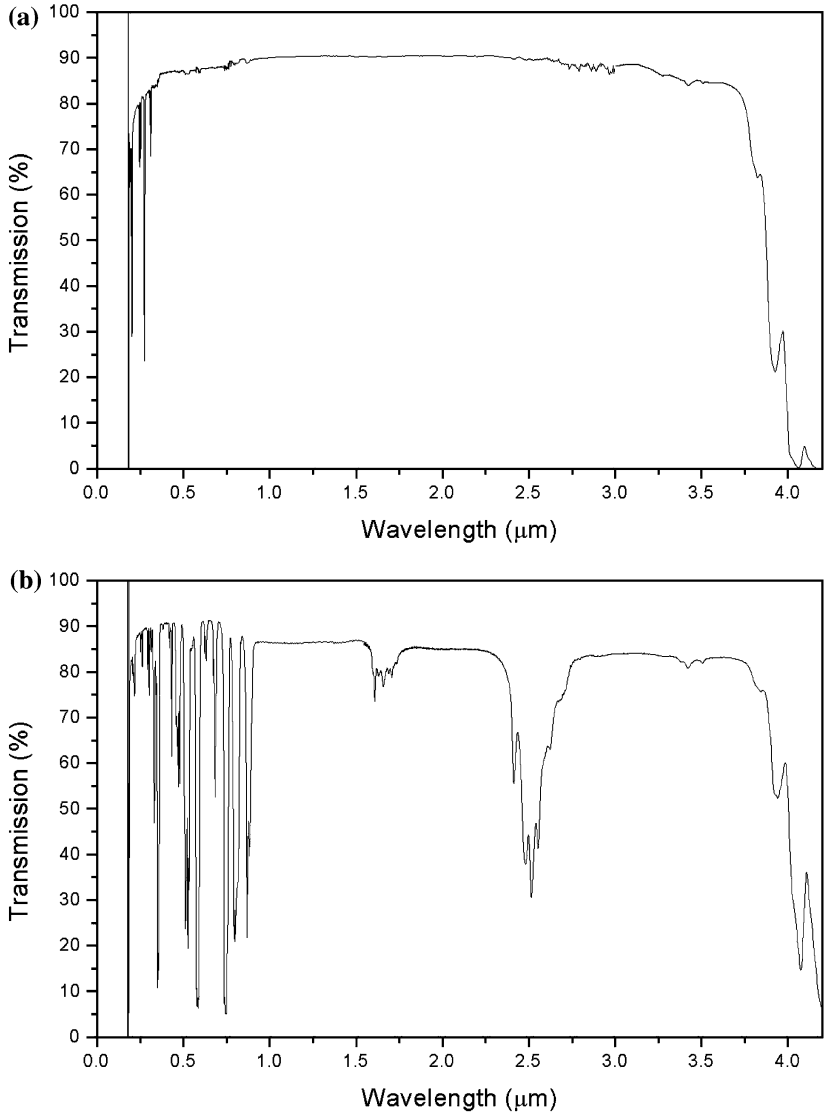

Figure 5. Transparency window of (a) KGP and (b) KNP at room temperature.

approximately 1, so we can confirm that the nonlinearity of KGP does not depend on any percentage substitution of Gd^{3+} by Nd^{3+}.

Conclusions

We determined the crystallization region of intermediate $KGd_{0.47}Nd_{0.53}(PO_3)_4$ and its saturation temperature isotherms, and we identified the neighboring phases found. All our results are consistent with the intermediate situation between KGP and KNP. The saturation temperatures and the number of neighboring phases are between those of KGP and KNP.

The crystal structure of type III KGP has been solved, and has been compared to that of the isostructural KNP. Because of the larger ionic radius of neodymium, when gadolinium was substituted for neodymium, all cell parameters increased except the β angle, which decreased slightly. Because the neodymium distribution coefficient for all compositions was almost 1, the high substitution acceptance of KGP has been proved, and KGP can be regarded as a promising laser host. Because of their noncentrosymmetrical structure, these materials can be used as nonlinear laser hosts

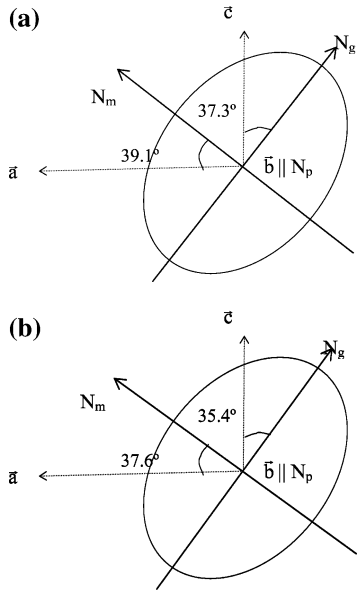

Figure 6. Optical ellipsoid of (a) KGP and (b) KNP in a projection parallel to [010] at $\lambda = 632.5$ nm and room temperature.

whose second harmonic efficiency is similar to that of KDP, and it maintains a constant value with Nd doping. Moreover, this material presents a significant low UV cutoff value (∼180 nm), which allows for the propagation of second and third harmonics of near-IR beams.

As a comparative study between KGP and KNP, we determined the optical tensor and ellipsoid. Few differences were observed between the optical frame orientations because the cell parameters are not very different. The refractive indices were also similar not only between themselves but also among the three principal optical directions.

Acknowledgment. The authors acknowledge financial support from the Generalitat de Catalunya under Projects 2001SGR317 and 2005SGR658 and Project 2003FI00770 (personal support) and from CICyT (Comisión inaterministerial de Ciencia y Tecnologia of the Spanish government) under Projects MAT-02-04603-C05-03 and MAT-05-06354-C03-02.

CM052114L